Weather Disturbances over Tropical Continents and Their Effects on Ground Conditions
Report No. 4

Surface-Air Energy Exchange over Eastern Venezuela as Related to Streamflow and Cumulonimbus Cloud Systems

By
David S. Renne'

Department of Atmospheric Science
Colorado State University
Fort Collins, Colorado

Colorado
State
University

Department of
Atmospheric Science

Paper No. 166

Surface-Air Energy Exchange over Eastern Venezuela

as related to Streamflow and Cumulonimbus Cloud Systems

by

David S. Renne´

Atmospheric Science Paper No. 166

Department of Atmospheric Science
Colorado State University
Fort Collins, Colorado

September 1970

ABSTRACT

Solar and net radiation measurements made during the Venezuelan
International Meteorological-Hydrological Experiment (VIM-HEX) con-
ducted in Venezuela in the summer of 1969 are discussed, and the
results presented in two separate parts of this paper.

In the first part it is shown that the average net radiation
surplus observed at the ground is converted to sensible and latent
heat transfer to the atmosphere. The sensible heat transfer can be
computed directly from morning and afternoon clear-day temperature
soundings. It is shown that the ratio of sensible to latent heat
transfer over eastern Venezuela during the study period is about
0.63. Based on the total energy balance at the earth's surface,
and dense rain-gauge measurements made over the study area, a stream
runoff of 0.07 cm/day per unit area is computed. This compares
quite well with the observed runoff per unit area of 0.09 cm/day.
It is concluded that single station meteorological measurements
coupled with areal rainfall data can give a first approximation to
the hydrology of a small tropical region over the time period of a
month or so.

In the second part of this report the radiation data is non-
dimensionalized by comparison with a standard, and the values are
located with respect to the center of an associated mesosystem
photographed by the VIM-HEX radar facility. The radius of the
observed radiation parameter from the center of the mesosystem is
also non-dimensionalized. In this reference system it is observed
that there is a sharp decrease in solar radiation and net radiation
within the mesosytem boundaries, and a rapid increase outside the
boundaries. It is concluded that the direct supply of energy from
the ground decreases toward the center of a tropical disturbance
over land and may vanish completely. In this respect the land-based
tropical cumulonimbus differs significantly from oceanic mesosystems,
where the supply of sensible and latent energy from the water actually
increases toward the center with very little diurnal control.

PART I

RIVER RUNOFF DETERMINATION FROM METEOROLOGICAL MEASUREMENTS

OVER A TROPICAL WATERSHED

Introduction

During the tropical meteorology experiment "VIM-HEX"[*] conducted in Anaco, Venezuela (9° N, 64° W), surface solar and net radiation measurements were part of the observing program. These measurements were desired (a) in conjunction with a computational approach for determining runoff from the watersheds in the area; and (b) for modeling energy exchange at the earth-air interface in relation to mesoscale convective cloud clusters over land. The two objectives will be discussed in sequence in the following.

The Problem of Runoff Determination

River runoff may be observed with stream gauges; alternately it may be computed from the energy balance at the earth's surface and precipitation measurements, with the assumptions of little underground runoff or moisture storage in the earth. It is clearly of interest to compare results from these completely independent techniques for reliability. If the latter can be demonstrated for relatively small riversheds or systems of such riversheds, weak or missing components of historical records of observations may be eliminated from consideration in determining at least gross aspects of the hydrology of such watersheds from a manipulation of meteorological and hydrologic observing systems. Further, the design of future observing systems should be affected and may be greatly simplified in some respects.

-----

[*] Venezuelan International Meteorological-Hydrological Experiment. This project was directed by Dr. Herbert Riehl of Colorado State University in the summer of 1969.

Procedure

Figure 1 shows the region of study in eastern Venezuela. Daily streamflow measurements were made from June through September, 1969 in the system of watersheds (as shown in Figs. 3 and 4) under the direction of Dr. Daryl B. Simons of Colorado State University. The charts indicate the locations of the gaging stations at the outflow end of all basins used in this study. The region can be characterized as a tropical savannah, consisting of open grasslands and widely spaced trees. Continuous radiation measurements were performed at Anaco, just outside the stream network, 14 August to 2 October, 1969. Surface observations of temperature and dewpoint, as well as daily radiosonde ascents, were also made at that site. A survey of short wave radiation over the watershed area by aircraft was undertaken on three days in order to determine whether radiation observations at Anaco could be considered as representative for the whole region. Visual inspection on daily streamflow measurement trips as well as continuous survey with weather radar was used to find out whether the watershed area had cloudiness significantly different from Anaco.

After applying small corrections, the net radiation balance at the surface was determined for the period 14 August to 2 October, 1969. The radiosonde ascents were used to establish the sensible heat flux, and the balance of the surface radiation excess was assigned to evaporation. From this information, plus a rainfall map for the area drawn on the basis of rain gage data, total stream discharge for the six weeks was computed and then compared with the direct discharge observations.

Instrumentation

The surface instrumentation, placed one meter above the ground, consisted of two Eppley pyranometers -- one measuring solar and diffuse sky radiation, and one measuring the reflected short wave radiation from the ground. A Suomi-type ventilated net radiometer measured the total flux of long and short wave radiation near the earth's surface. All three radiation parameters were continuously
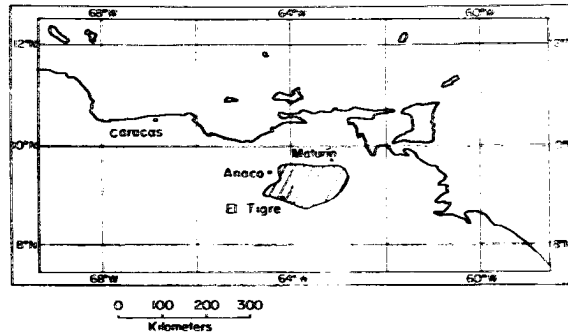
Figure 1.   Northern coast of South America.   The hatched area
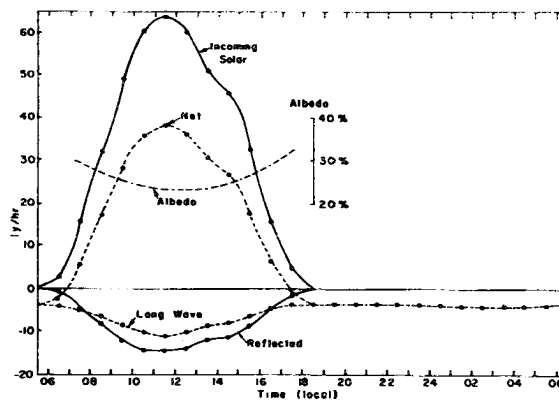outlines the system of watersheds utilized in the VIM-HEX study.

Figure 2.   Mean hourly values of the radiation parameters measured
at Anaco, Venezuela for the period 14 August to 2 October, 1969.

recorded on a strip chart. Subsequent data reduction yielded mean hourly values of the net radiation, the incoming solar radiation, and the reflected solar radiation. From these values the albedo and the net infrared flux were also computed.

The aerial survey was provided by a Queen-Air aircraft for the National Center for Atmospheric Research (NCAR) in Boulder, Colorado. This aircraft, instrumented with two high-response Eppley pyranometers, made measurements of the variations in solar and reflected radiation over the entire region.

Components of the Radiation

All radiation parameters were averaged for each hour of the day over the entire period of study. It should be noted that a "day" is defined here as starting at 0600 on one morning, the first hour in which solar radiation is recorded, and ending at 0600 the following morning.

The intensity of incoming short wave radiation increases steadily to a maximum about one hour before local noon -- the approximate time of onset of large scale convection (Fig. 2). Thereafter it decreases. The total daily average of solar radiation, 433 ly, compares well with that measured at two Venezuelan observatories, Observatorio Cagigal (10.5° N, 66.9° W) and La Orchilla (11.8° N, 66.2° W). These reported average insolation of 409 ly/day and 459 ly/day, respectively (Boletin Climatologico, 1969), for the period of measurement at Anaco.

The reflected radiation, plotted as negative numbers in Fig. 2, follows the same pattern as the incoming radiation. The albedo curve, expressed as a percentage of the ratio of incoming to reflected short wave radiation, is strikingly concave, reaching a minimum value around local noon, and increasing with zenith angle. Budyko (1968) arrives at a similar albedo profile; he explains it as the variation in reflectivity characteristics with zenith angle of a rough soil surface covered with vegetation. The minimum albedo is 22.7% during the hour before noon, and the net for the day, based on the total daily values of incoming and reflected short wave radiation, is 24.7%

TABLE I

Average Radiation Balance at Surface
(ly/day)

	All Days	Dry Days	Wet Days
Short Wave Radiation Reaching Ground	433	456	393
Less Reflected Radiation (Albedo 24.7%)	-107	-112	- 97
Net Radiation Absorbed in Ground	326	344	296
Less Long Wave Radiation	-130	-133	-125
Net Radiation	196	211	171

Adjustment

Reflected Radiation (20% albedo)	87	91	79
Net Radiation Absorbed (adjusted for 20% albedo)	216	232	199

The net radiation curve in Fig. 2 follows the same course as solar radiation during the day. However, it becomes positive about one hour after sunrise and negative one hour before sunset. The 24-hr integrated value is +196 ly. Using these data it is now possible to compute the net long wave radiation, and therewith all radiation components, with the formula

$$N = (1 - a)S + L_n \qquad (1)$$

where N is net radiation, S short wave radiation, a the albedo, and L_n the net infrared radiation. From Fig. 2, L_n is always negative, almost uniform during the night and largest in the noon hours when the earth's surface is hottest.

Table 1 summarizes all radiation components and the net daily radiation storage as measured at Anaco. It is seen that only 40% of the radiation absorbed in the ground is radiated back to space. This result happens to be in good agreement with London's (1957) computations for the whole latitude belt 0-10° N in summer. Further, London calculated the net long wave radiation for this belt as 131 ly/day; Budyko (1962) computed a net radiation storage of 197 ly/day for tropical continents 0-10° N. The close agreement between single station data and large area estimates must, of course, be considered as coincidental, at least to some extent.

Aerial Albedo Measurements

Since cloudiness over Anaco and the watersheds to the east was nearly the same, it is plausible that the values of S and N determined at Anaco may be applied over the whole study area. A systematic difference, however, may exist in albedo, since the vegetation of Anaco is open savannah type, while at least part of the watershed area is forested. As already mentioned, two aerial research missions were carried out by an NCAR Queen-Air aircraft instrumented to measure both incoming and reflected short wave radiation. Should the area-averaged albedo turn out different from that at Anaco, an adjustment in net energy storage could be made by applying a correction factor.

The aircraft flew at constant altitude about 500 feet below cloud base (2,000 feet above the ground). Both flights were made during the period of high zenith angle so that the diurnal variation in albedo would not affect the readings during the course of the flight, and so that the late afternoon cloudiness that often occurs would not be a factor. The flight plans were designed so that a coverage of the area was obtained during each flight, with several cross-over points to check short-period albedo variations.

Figures 3 and 4 give the albedo analyses based on the two flights. Albedo varied by several percent from one day to the next, mainly due to minor changes in cloud cover. In addition, albedo changed by as much as 4% at the cross-over points on the individual flights. The pattern is not consistent from one day to the next, suggesting control by cloud arrays rather than surface features. Nevertheless, it is apparent that albedo does not vary by more than 6% over the bulk of the area.

In spite of minor differences, both days with aircraft missions may be classified as "dry" days, with hardly a radar echo over the area. Unfortunately, the flights had to be scheduled prior to installation of the surface radiation instrumentation. They may, however, readily be compared with the radiation balance for "dry days" at Anaco as given in Table 1 and discussed more fully later in this report. Table 2 shows the comparison. The aircraft measurements and the surface measurements of solar radiation differ very little; but the albedo measured by aircraft is considerably less than that obtained at our surface site. Two possible reasons may be cited. First, the Anaco site was located on an open grassy field which would give a characteristically higher albedo than heavily forested regions included in the aircraft overpasses. Second, since the aircraft was 2,000 ft above the ground, the down-facing pyranometer was "seeing" both sunlit and shaded areas due to the scattered cloud cover of about 3/10 low cumuli present.

Budyko (1958) gives the albedo of rainy season savannah as 18%, which is slightly higher than that measured by the aircraft. The Anaco albedo of Table 1 compares with Budyko's dry season value of
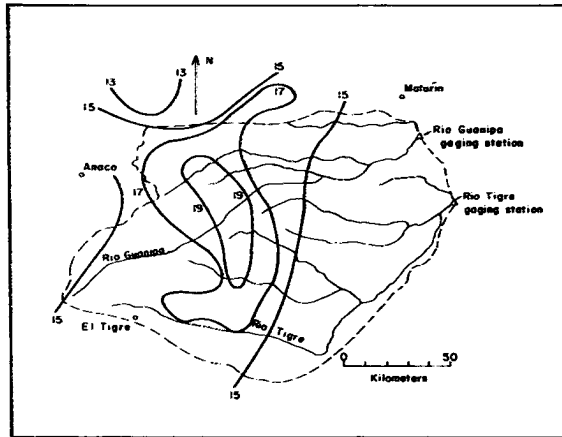
Figure 3.   Analysis of albedo in per cent as measured by the NCAR Queen-Air over the system of watersheds, 29 July, 1969.   Included are the major rivers and gaging stations used in this study.
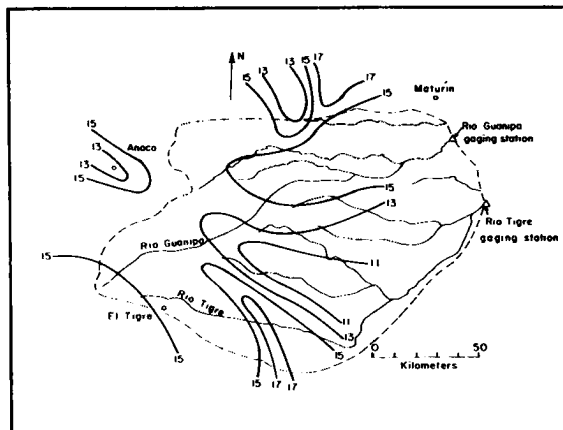

Figure 4.   Same as Figure 3 only for 30 July, 1969.

TABLE 2

Comparison of Queen-Air Radiation Values

With Mean Surface Radiation Measurements at

Anaco, Venezuela on Dry Days

Date and Local Time	Solar Radiation (ly/hour)	Reflected Radiation (ly/hour)	Albedo (per cent)
29 July 1969 Queen-Air 1100 - 1400L	61.2	10.6	17.3
Anaco (Dry Days) 1100 - 1400L	62.2	14.2	22.8
30 July 1969 Queen-Air 1100 - 1300L	67.1	10.5	15.6
Anaco (Dry Days) 1100 - 1300L	64.8	14.6	22.6

25% even though the measurement was made in the wet season. Based on this evidence the albedo may have been overestimated at our site, as far as a representative area value is concerned.

It was concluded that the truth was somewhere between the possibilities cited, and an average albedo of 20% was adopted. Fortunately, the exact correction is not important since we are dealing with a small percentage of a small term. The net radiation for the 20% albedo is given in the lower portion of Table 1. It is seen that the increment in N amounts to only 10%, well within range of calculation accuracy that can be hoped for. The same order of variation occurs over the area as seen from the albedo counts.

Sensible Heat Transfer

Assuming that the temperature of the ground remains constant, the net energy storage in the ground must be given up to the atmosphere through the well known mechanism stated by

$$N = Q_s + Q_e \tag{2}$$

where Q_s and Q_e are sensible and latent heat transfer from earth to atmosphere, respectively. This formula is thought to hold closely over land in any 24-hr interval, in contrast to the oceans, based on the radiation balance computed from Nimbus III satellite overpasses (Raschke, et.al., 1970).

Much attention has been given in the literature to the partitioning of N and to the ratio Q_s/Q_e. The sensible heat transfer Q_s may be determined approximately from early morning and early afternoon temperature soundings, near minimum and maximum surface temperature conditions, if horizontal and vertical advection of heat are small and if no evaporation from falling rain occurs below cloud bases, i.e. on fair weather days. In this type of situation, the rise of temperature from minimum to maximum can only be due to conduction heating from the ground below cloud base. The following equation for energy balance in the sub-cloud layer applies:

$$C_p \int_{min}^{max} \frac{\partial T}{\partial t} dt \int_{P_o}^{P} \frac{\delta P}{g} = \int_{min}^{max} Q_s dt + \int_{min}^{max} \int_{P_o}^{P} \frac{\partial}{\partial P}(1-aS)\frac{\delta P}{g} dt - \int_{min}^{max} \int_{P_o}^{P} \frac{\partial}{\partial P}(L_n)\frac{\delta P}{g} dt \tag{3}$$

In (3) the first term on the left represents the total heat gained in the sub-cloud layer, where C_p is specific heat of dry air, T is temperature, δP the pressure thickness of the layer from the surface, P_0 to cloud base P; and g is the acceleration of gravity. The integral from "min" to "max" represents integration in time t from the morning minimum to the afternoon maximum surface temperature. The first term on the right of (3) represents the transfer of sensible heat into the sub-cloud layer, the second term represents the convergence of short wave radiation and the third term the convergence of long wave radiation. The sign change takes into account the reversal in direction of long wave flux from short wave flux.

Equation (3) may now be solved explicitly for Q_s. There were five clear days in Anaco when temperature soundings for both the early morning minimum temperature conditions and the afternoon maximum temperature conditions were available. Since net radiation is still positive after the afternoon temperature maximum, it is assumed that any excess Q_s transfer into the air after this time is balanced by a corresponding heat loss transfer toward the ground at night. Fig. 5 shows the temperature soundings of one of the clear days used in the study, 4 September, 1969. It is clear that the assumptions mentioned above are valid for this particular case, since the two curves intersect at cloud base and there is very little change in the two soundings above cloud base. The stippled area, then, represents the heat added to that layer from the processes indicated on the right hand side of (3).

In equation (3) the convergence of short wave radiation was taken from climatological values given by Yamamoto (1962). For latitude 9.4° N between July and October it is estimated that the total short wave absorption in the boundary layer amounts to 0.65° C per day, or, for the time period considered here, about 0.40° C per day.

The long wave convergence was established by a numerical Elsasser-type computation reported by Dr. Pete Kuhn of Environmental Science Services Administration Laboratories, Boulder, Colorado.*
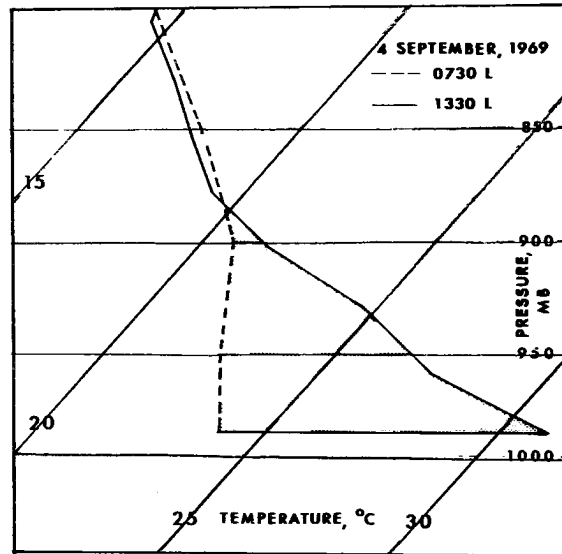
---

* Personal communication.

Figure 5. Temperature soundings plotted on a low-level tephigram for 0730 and 1330 local time (the approximate times of surface minimum and maximum temperature conditions) for 4 September, 1969. Since the two curves intersect approximately at cloud base, and since there was very little temperature change above cloud base, the stippled area represents heat added to the sub-cloud layer due to sensible heat transfer and convergence of short and long wave radiation.

Based on sample computations, it was established that in the after-
noon, with strong surface heating, there is actually a net conver-
gence of infrared radiation which largely counteracts the early
morning or late evening observed divergence of infrared radiation
in the boundary layer (e.g. Riehl, 1962 and Cox, 1969a). Thus it was
assumed that over the period of interest the average convergence of
long wave radiation is zero.

Table 3 gives the result of evaluating equation (3) for 5 clear
days during the study period. It is seen that Q_s ranged from 76 to
97 cal/cm^2. The average temperature increase for the sub-cloud layer
of 100 mb thickness was near 3.5°C, and this must also be the temper-
ature loss from long wave radiation in the layer during the night.

Evaporation
___

We can now evaluate Q_e in equation (2), noting that Q_e = LE,
where L is latent heat of evaporation and E evaporation, if density
of water is taken as 1 g/cm^3. Values of N, E and also of Q_s/Q_e are
contained in Table 4. The average evaporation per unit area of
0.24 cm/day is considerably lower than oceanic evaporation of 0.35
to 0.50 cm/day in the tropics; correspondingly, the ratio Q_s/Q_e is
much higher.

Since only clear days were used for computing Q_s, the average
heat storage and therefore Q_e are somewhat overestimated as far as
averages for the 45-day period are concerned. For determining a
more representative value we can re-write equation (2) as

$$Q_e = \frac{N}{(1+Q_s/Q_e)} \qquad (4)$$

Assuming Q_s/Q_e = 0.63 from Table 4, a constant, and using the adjusted
value of N = 216 cal/day from Table 1, then E = 0.23 cm/day, only
slightly lower. Even with the unadjusted value of N = 196 cal/day
in Table 1, E = 0.21 cm/day, still within range of error of all
calculations. For comparison, Budyko (1962) quotes E = 0.22 cm/day
for all land masses between 0-10° N and 0.21 cm/day for the South
American continent (Budyko 1963), surprisingly close.

TABLE 3

Computation of Q_S from Equation (3)

Date and Local Time	$C_P \iint \dfrac{\partial T}{\partial t} dt \dfrac{\delta P}{g}$ cal/cm^2	$\iint \dfrac{\partial}{\partial P}(1-aS) dt \dfrac{\delta P}{g}$ cal/cm^2	Q_S cal/cm^2
4 September 0730 – 1330	97	8	89
18 September 0730 – 1300	91	8	83
20 September 0730 – 1500	105	8	97
25 September 0730 – 1100	84	8	76
30 September 0730 – 1400	98	8	90
Average	95	8	87

TABLE 4

Computation of Evaporation

Date	N (cm/cm^2)	E (cm/day)	Q_s/Q_e
4 September	238	0.25	0.60
18 September	204	0.21	0.68
20 September	237	0.24	0.69
25 September	250	0.30	0.44
30 September	199	0.19	0.82
Average	225	0.24	0.63

Computed and Observed River Discharge

As indicated in the Introduction, observed river discharge will be compared with computed discharge using the relation

$$\text{Runoff} = P - E \qquad (5)$$

where P is precipitation. This relation assumes (a) that moisture storage in the ground is small, probably correct in the later parts of the rainy season; and (b) that underground discharge may be neglected. This latter assumption appears to be quite valid over all except the southern reaches of the study area, based on the low infiltration rates and permeability of the soil observed by the hydrologists (Holland, 1970).

The precipitation chart (Fig. 6) shows a surprisingly complex pattern for the accumulation of 48 days' rain over terrain that is relatively flat, with a drop of about 200 meters from the west to the eastern boundaries of the study area. Consequently, an isohyetal analysis is difficult. Averaging of Fig. 6 yields P = 0.30 cm/day per unit area, a value that will be used but that at best can be considered accurate to better than 10% in view of the uncertainty in drawing isohyets. Given the above value of P and E = 0.23 cm/day, the runoff per unit area is 0.07 cm/day.

Nearly all outflow from the drainage area was measured by the two stream gages located on the Rio Guanipa and the Rio Tigre at the exit from the study area. The discharge from these two rivers averaged 119 m^3/sec. Given the drainage area of 1.11×10^4 km^2, the average observed runoff depth per unit area is 0.09 cm/day, slightly more than the computed value. It may be concluded that good agreement between computed and observed discharge has been obtained within all computational and observational limitations, indicating that the computational route is feasible for a first approximation of water balance in relatively small drainage areas and over a time period of about a month. It is of interest that the discharge is only 25-30% of the precipitation in the middle of the rainy season in a portion of the equatorial rainfall zone.
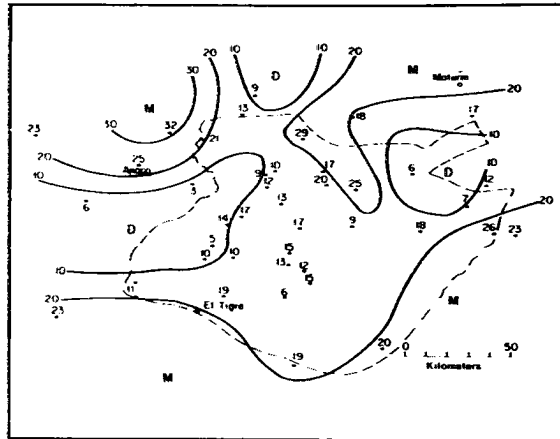
Figure 6.   Total rainfall in centimeters for the period 14 August to 30 September, 1969. M (moist) represents centers of high and D (dry) of low rainfall.

Finally, it is worth mentioning that surface climatological data from one or a few stations including a net radiometer may furnish an abbreviated method for a first estimate of stream discharge over tropical plains where the assumptions made in the report essentially apply. The main problem is determination of Q_S. We may try the relation

$$Q_S = \frac{C_p}{M}\left(\frac{T_{max}-T_{min}}{2}\right) \tag{6}$$

where T_{max} and T_{min} are measured in the thermometer shelter, M is the mass of the atmosphere below cloud base per unit area, and $T_{max}-T_{min}$ is allowed to decrease linearly from the surface value to zero at cloud base. This computation is suggested from Riehl and Malkus (1958), who showed that sensible heat transfer from the ground to the air within the equatorial trough zone is much higher than originally expected, due, in part, to the diurnal range of temperatures. In eastern Venezuela, $T_{max}-T_{min} \doteq 10°$ C and M = 100 g/cm with a cloud base 1 km above the ground. Then (6) yields Q_S = 120 ly/day, an overestimate compared to the data of Table 3 mainly due to shallow nocturnal temperature inversions near the ground. The correction factor is 3/4 for eastern Venezuela; it can be determined climatically from radiosonde observations for all tropical areas.

PART II

MODELING OF ENERGY EXCHANGE AT THE SURFACE

OF TROPICAL MESOSCALE DISTURBANCES

Introduction

This part of the investigation was prompted by the expectation
that surface interaction in cumulonimbus systems over land must be
completely different than over sea, leading to marked differences in
the life cycle of these cloud conglomerates. Over sea, Q_s and Q_e
should reach maxima (Riehl and Malkus, 1958) that may attain values
several times the solar constant, drawing on energy storage in the
sea over days or weeks. Such local energy addition to the meso-
systems may prolong their life and lead to continual renewal. In
contrast, energy penetration into the ground is known to be limited
to the uppermost centimeters. Most energy absorbed by the ground is
immediately returned to the atmosphere through conduction heating
and evaporation. This is shown by computations of the radiation
balance from Nimbus III satellite overpasses (Raschke, et. al, 1970).
Hence, ground-air energy exchange should affect the life cycle of
cumulonimbus systems in quite a different way than over sea, namely
through introduction of a strong diurnal period, in the course of
which energy transferred from ground to atmosphere over large areas
would become concentrated in localized cloud towers. The latter,
however, would receive very little or no energy directly from below
during their existence. The diurnal period, well known from most
tropical continental areas, was found to be especially strong over
eastern Venezuela. The forenoon was nearly always rainless and most
convective activity compressed into the late afternoon and early
evening hours (as will be shown in Figs. 9 and 12), a rhythm main-
tained even in the strongest synoptic disturbances. In contrast,
traveling disturbances do supercede the diurnal period in many other
tropical areas; secondary and even primary maxima of nocturnal pre-
cipitation are encountered, often without good explanation. It is

hoped that the eastern Venezuela study will assist in solving the more complicated problems of other regions by providing contrast.

Surface Energy Balance on Dry and Wet Days

First, the influence of synoptic disturbances on the daily course of all radiation parameters will be determined. The 46 days with complete radiation records were divided into "undisturbed" and "disturbed" days, better dry and wet days in view of the method adopted for classifying days. A "wet" or "disturbed" day was defined as a day which contributed more than 1% to the total precipitation in the whole area shown in Fig. 6. It turned out that there were 30 dry and 16 wet days.

The radiation parameters were averaged separately for dry and wet days. Fig. 7 shows there is virtually no difference prior to 11 a.m., while in the afternoon incoming radiation was reduced as much as 20% in the mean. Oddly enough, the albedo did not differ between dry and wet days. Net radiation absorbed in the ground, as well as long wave radiation from the ground, were smaller on wet days during afternoons than on dry days (Fig. 8). Nighttime differences were small, but the outgoing radiation averaged slightly lower on the days with more moisture and cloud cover. The differences of the daily sums are given in Table 1. Figs. 7 and 8 show that these differences result almost entirely from the afternoon hours. It is apparent that the direct energy supply of these disturbances from the ground decreases as the cloudiness and precipitation increases. On the other hand, it is of interest that the frequency as well as the greatest extent of mesoscale systems occurs when the total accumulation of solar energy in the ground has taken place and presumably been made available to the atmosphere (Fig. 9).

Surface Radiation Energy Exchange in Relation to Mesoscale Systems

It was desired to obtain the distribution of net energy absorbed by the surface in coordinates fixed with respect to the mesoscale systems. Such a distribution would indicate the gradient of energy
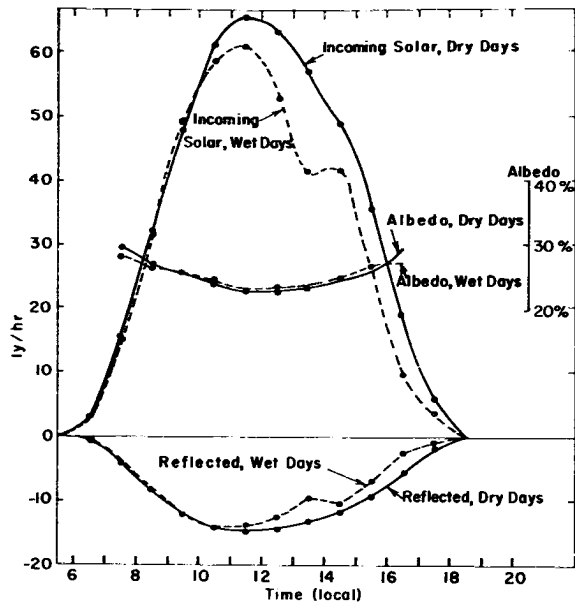
Figure 7.   Mean hourly values of the incoming and reflected solar radiation, also albedo in per cent, for the two categories; wet and dry days separately.
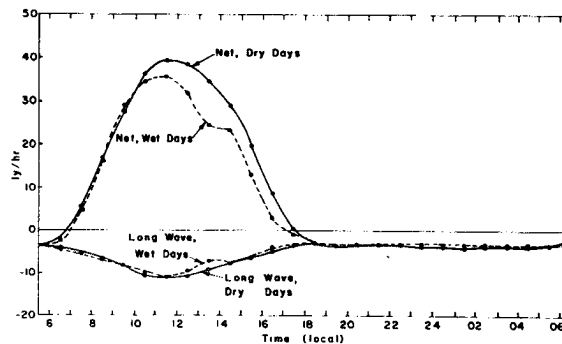

Figure 8.   Mean hourly values of net and long wave radiation for the two categories; wet and dry days.
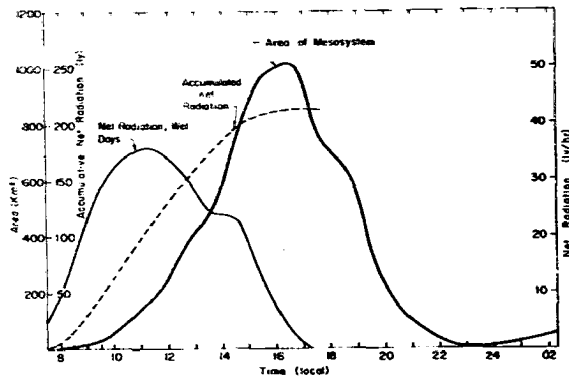
Figure 9.   Hourly march of the average mesosystem area, the average net radiation for wet days, and the accumulated net radiation for wet days measured at Anaco, Venezuela for the period 14 August to 2 October, 1969.

available for transfer to the atmosphere from the center of meso-
systems outward and could serve as a model in studying the role of
the differential energy transfer from ground to atmosphere on the
life cycle of mesosystems.

The technique was to plot the radiation values at Anaco averaged
for one hour on x-y horizontal coordinates where the origin of the
coordinate system lies in the center of a radar echo. This method
is similar to the one used by Cox (1969b) for studying radiation
characteristics of mid-latitude synoptic features. In the present
study, however, various normalization procedures had to be adopted.

Echo Area. A mesosystem was defined as an echo or cluster of
echoes with area greater than 400 km^2 at maturity (Riehl and Malkus,
1958). Some echoes were much larger, and all went through a life
cycle in size, as is well known. In order to make different echoes
comparable for a composite plot, the area had to be normalized.
This was done by adopting a non-dimensional horizontal distance
scale with a value of one at the outer edge of the echo averaged
over a representative segment of arc. In the following illustrations,
therefore, all points at radius less than one lie inside the echo
area and all points outside are spaced for equal increments in radius.
The procedure implies that mesosystems have a decay function of
influence proportional to their echo area.

Time of Day. Since data were insufficient for producing charts
at hourly or two-hourly increments of local time, a method had to be
found to eliminate the diurnal variation of radiation. For this
purpose, a "standard" diurnal variation of radiation was developed
as follows. From a frequency distribution of the daily sums of in-
coming solar radiation (Fig. 10), the hourly values of all radiation
parameters were separated for the days with total incoming radiation
greater than 400 ly and averaged. Fig. 11 shows the result, which
is not identical with Fig. 7, although differences are small. All
individual hourly radiation data were then expressed as per cent
deviations from the curves in Fig. 11 and plotted. Much scatter
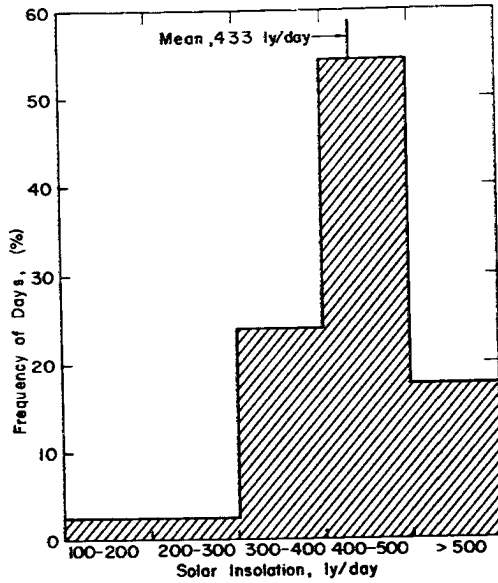resulted from the many echoes after 1600L occurring at low values

Figure 10.   Frequency distribution of the total daily solar radiation measured at Anaco, Venezuela for the period 14 August to 2 October, 1969.
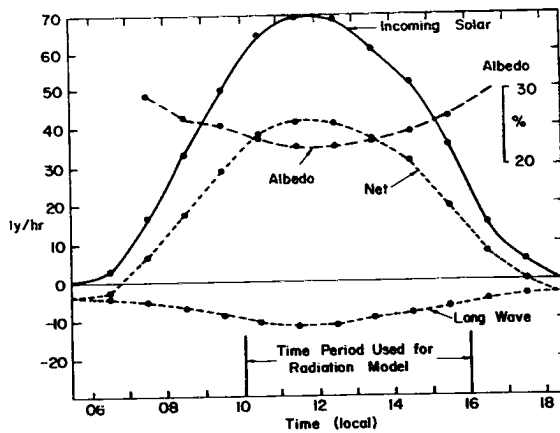

Figure 11.   "Standard" radiation values based on all days with a total daily solar radiation greater than 400 langlies. Included is the time period utilized for the radiation model in this study.
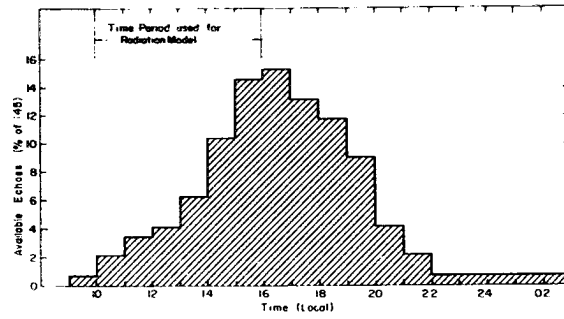
Figure 12. Frequency distribution of the hourly occurrence of the 145 radar echoes available for this study. Included is the time period actually utilized for the radiation model.

of incoming radiation. Evidently, the local gradient of radiation plays only a very minor role in these late afternoon clouds. They were therefore eliminated from the statistic, although this represented a large loss of data -- 90 echoes out of 145 were dropped leaving only 55 for further analysis (Fig. 12).

Other Normalization Attempts. The coordinate system was rotated in the direction of echo propagation in order to preserve asymmetries arising from storm displacement. In another attempt, the coordinates were rotated into the direction of the velocity shear vector from 500 to 200 mb, thought to normalize anvil positions. Neither or these rotations reduced the scatter of the data. Account was also taken of the fact that the single station, Anaco, would experience a different sun angle with respect to an echo in a given position at different times of day. For instance, with an echo to the west, the station would be more likely to receive radiation in the early part of the day than in the afternoon. No positive results were obtained. It would appear that clouds are too individualistic to permit themselves to be parameterized two-dimensionally, based on this limited measuring capability. However, one-dimensional parameterization -- data plotted as a function of the non-dimensional radius alone -- proved feasible; results are presented below.

Radiation Parameters as Function of the Echo Radius

Incoming Solar Radiation. Figure 13 shows a frequency distribution to the deviations of incoming solar radiation from the mean, as well as means and medians, at radial intervals from 0 to 1, 1 to 2, and greater than 2. Inside the echo area, about 70% of the solar radiation was intercepted by the cloud cover. A reduction of 100% was never quite attained. On the other hand, in cases with broken echo cells, radiation not far below the standard value was recorded. At the radial interval from 1 to 2, normal clear-day incoming radiation was quickly attained and outside the radius of 2 half of the values exceeded the standard, suggestive of subsidence outside of echo centers, although such subsidence could never be assigned to any particular sector with respect to the moving mesosystem.
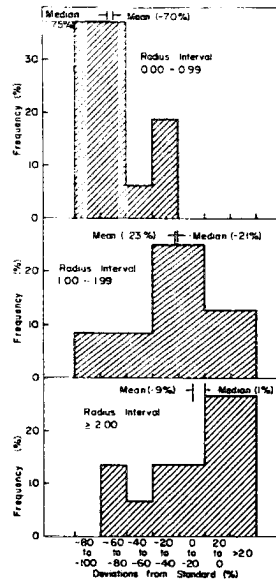
Figure 13.   Frequency distributions of the occurrence of per cent deviations of solar radiation from standard for various non-dimensional intervals of all mesosystems (1.00 is the boundary of the mesosystems).
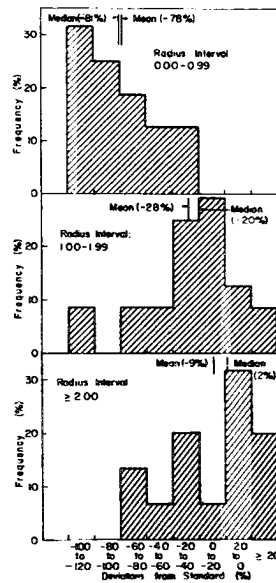

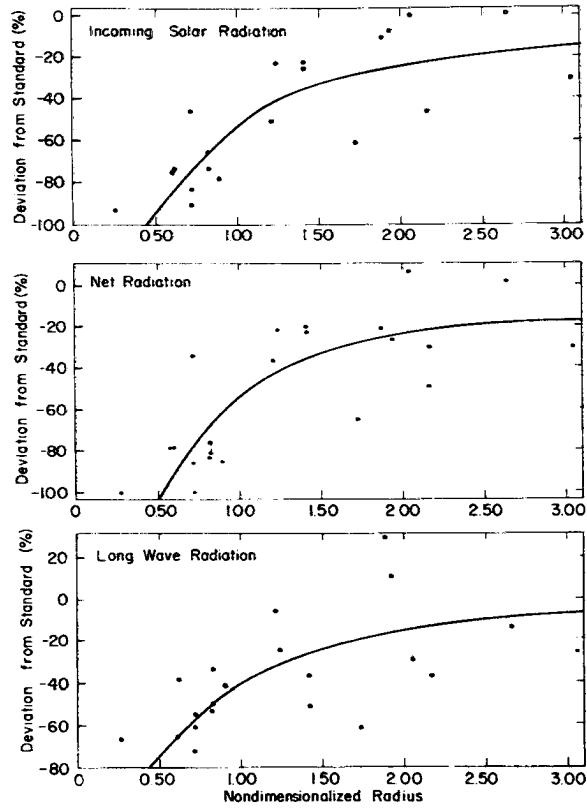Figure 14.   Same as Figure 13 only for per cent deviations of net radiation from the standard.

Figure 15.   Scattergrams of per cent deviations vs non-dimensionalized radius for the various radiation parameters for the time period 1000-1400 local.   The line of best fit has been drawn freehand.

Figure 14 contains frequency distributions of net radiation
received at the ground, arranged similar to Fig. 13. The pattern
also follows Fig. 13. Inside the echo areas the net energy supply
to the ground vanished almost entirely and even became negative in
extreme cases when outgoing exceeded incoming radiation. Outside
the radius of 2 more than average net absorption of heat occurred
for half of the cases. If it may be assumed that energy transfer
from ground to atmosphere is proportional to net energy received by
the ground in view of the ground's very low storage capacity, then
Fig. 14 brings out the main difference between continental and
oceanic cumulonimbus; over the oceans the gradient of energy supply
to the mesosystem would be exactly inverse to that of Fig. 12.

Figure 15, finally, gives profiles of incoming solar radiation,
of net radiation absorbed and also of long wave radiation emitted
from the ground for 21 cases between 1000 and 1400L, when solar
heating is at its maximum. When the sample is so restricted, the
positive values outside the radius of 2 no longer occur. It is seen
that, despite considerable scatter, reasonable continuous profiles
of all three quantities could be drawn.

Conclusion

It is clear that an attempt has been made here to maximize the
information drawn from very limited observing capability. A large
experiment with numerous surface radiation stations, aircraft
traverses, etc. would, no doubt, provide a better picture. However,
it appears doubtful whether such an experiment would negate the basic
results of Figs. 13, 14 and 15, which are entirely in line with antic-
ipation. It is believed reasonable to suggest that the diagrams of
this report give first order approximations of the actual state and
that they bring out correctly the difference in surface interaction
between oceanic and continental mesosystems.

Figures 13, 14 and 15 demonstrate that there is a large reduction
in solar radiation and of heat available for evaporation and sensible
heat transfer from ground to atmosphere within the boundaries of a
tropical continental mesosystem. The gradient of such energy exchange

is directed outward, whereas over the ocean it is directed inward. Further, the occurrence of mesosystems over land is largely controlled by the diurnal surface heating cycle in eastern Venezuela, more so than over some other continental areas of the tropics and certainly in contrast with the ocean where the surface heat supply is essentially independent of the time of day. The importance of this difference should not be underestimated, even though it can be demonstrated that local evaporation contributes at best one-tenth to the rain derived from a cumulonimbus. In hurricanes, the small addition of energy from the sea furnishes the whole mechanism for creation and maintenance of the warm core (Riehl and Malkus, 1961, Riehl, 1963) and a similar argument can be advanced for the mainte- and regeneration of cloud clusters in other types of synoptic disturbances over sea. Outside of downdraft areas, low clouds with base near 2,000 ft remain readily available over sea for a start of new build-ups, whereas over eastern Venezuela all low clouds died away subsequent to overturning of the atmosphere in the afternoon, the cloud base generally rose to about 15,000 ft and low clouds only reappeared the next morning under the stimulus of surface heating from freshly received sunshine.

Occurrence of the peak of radar echoes lags the peak of incoming radiation by about 5 hours, but coincides well with the time of total energy absorption during the day, that is near sunset. Thus continental cumulonimbus appear to be related to the gross accumulation of energy over large areas, which can then be concentrated in small regions of ascent independent of any local energy source underneath the cloud. Further analysis of these relations, their connection with large-scale stability trends, broad ocean-continent mass exchange and the semi-diurnal pressure wave, is outside the objectives of this study.

ACKNOWLEDGEMENTS

REFERENCES

Boletin Climatologico, Republica de Venezuela, Comandancia General de la Marina, Dirrecion de Hidrografia y Navegacion, Observatorio Naval "Juan Manuel Cagigal", Division de Meteorologia, Seccion de Climatologia, August and September, 1969.

Budyko, M. I., 1958: The Heat Balance of the Earth's Surface, Office of Technical Services, Washington (Translated from Russian).

Budyko, M. I., 1963: Atlas Teplovogo Balansa, Gidrometeorologicheskoe Izdatel'skoe, Leningrad.

Bubyko, M. I., et. al., 1962: The Heat Balance of the Surface of the Earth, Sov. Geograph, 3, 3-16.

Cox, S. K., 1969a: Observation Evidence of Anomalous Infrared Cooling in a Clear Tropical Atmosphere, J. of Atmos. Sci., 26(6), 1347-1349.

Cox, S. K., 1969b: Radiation Models of Mid-latitude Synoptic Features, Mon. Wea. Rev., 97, 637-651.

Holland, M. E., 1970: Soils and Infiltration Data, Colorado State University, (to be published).

London, Julius, 1957: A Study of the Atmospheric Heat Balance, Final Report, Project 131, New York University Department of Meteorology and Oceanography, New York.

Raschke, E., T. H. Vonder Haar, W. R. Bandeen, and M. Pasternak, 1970: The Radiation Balance of the Earth-Atmosphere System During June and July 1969 from Nimbus III Radiation Measurements - Some Preliminary Results, Contribution (A 2.3) to COSPAR XIII, Symposium on Remote Sounding of the Atmosphere, Leningrad, U.S.S.R., 20-29 May, 1970.

Riehl, H., 1962: Radiation Measurements over the Caribbean During the Autumn of 1969, J. Geo. Res., 67(10), 3935-3942.

Riehl, H., 1963: Some Relations between Wind and Thermal Structure of Steady State Hurricanes, J. Atmos. Sci., 20(4), 276-287.

Riehl, H., and J. S. Malkus, 1958: On the Heat Balance in the Equatorial Trough Zone, Geophys., 6, 503-538.

Riehl, H., and J. S. Malkus, 1961: Some Aspects of Hurricane Daisy, 1958, Tellus, 13, 181-213.

Yamamoto, Giichi, 1962: Direct Absorption of Solar Radiation by Atmospheric Water Vapor, Carbon Dioxide, and Molecular Oxygen, J. Atmos. Sci., 19(2), 182-188.